Si-doped Polycyclic Aromatic Hydrocarbons: Synthesis and Opto-electronic Properties

Thomas Delouche,[a] Ghizlene Taifour,[a] Marie Cordier,[a] Thierry Roisnel,[a] Denis Tondelier,[b] Payal Manzhi, [b,c] Bernard Geffroy,[b,c] Boris Le Guennic,[a] Denis Jacquemin,*[d] Muriel Hissler,[a] Pierre-Antoine Bouit*[a]

We report the straightforward synthesis of Si-containing PAHs. The impact of π-extension and exocyclic modifications on both the optical and redox properties is investigated using a joint experimental/theoretical approach. By taking advantage of the solid-state luminescence of these derivatives, electroluminescent devices are prepared. Such preliminary optoelectronic results highlight that these heteroatom-containing PAHs are promising building blocks for organic electronics.

Polycyclic Aromatic Hydrocarbons (PAHs) are organic compounds consisting of ortho- and peri-fused aromatic rings.[12] These derivatives appeared during the last years as efficient semi-conductor in a wide range of application linked with the plastic electronic (Organic Solar Cells (OSC), Field-Effect Transistors, organic batteries, etc.). Various strategies have been used to tune their molecular properties and consequently the device performances. One of them is to modify the C-$sp2$ skeleton by introducing various ring-sizes (5, 6 or 7-membered rings) or edge configuration (armchair, zigzag, cove, etc.).[3] Another approach is to introduce heteroatoms into the C-scaffold,[4] a strategy successfully applied to second row heteroatoms such as B,[5] N,[6] O.[7] While the insertion of third row elements such P also proved to be a valuable molecular engineering strategy,[8] there are surprisingly few examples of Si-containing PAHs. This is rather surprising considering the important role played by siloles (5-membered unsaturated Si-heterocycles) oligomers and polymers in opto-electronic applications, and notably OSCs.[9] Such devices benefit from the low lying LUMO of the silole.[10] Moreover, the possibility to prepare stable derivatives with unusual coordination number (hyper-[11] or hypo-coordinated[12]) or displaying π-single bonding[13] make organosilicon derivatives very original scaffolds for π-conjugated system engineering. In order to take advantage of the presence of heteroatoms in PAHs, the main challenge is to find efficient synthetic pathway compatible with both the preparation of large C-sp2 framework and the presence of the heteroatom(s). Until now only few "Si-compatible" approaches toward Si-doped PAHs A-D (Fig. 1) have been developed including Sila-Friedel-Crafts reaction,[14] transition-metal catalysis,[15] and dehydro-Diels-Alder[16]. For this reason, the study of the opto-electronic properties of the resulting Si-containing PAHs is clearly underexplored.[17]
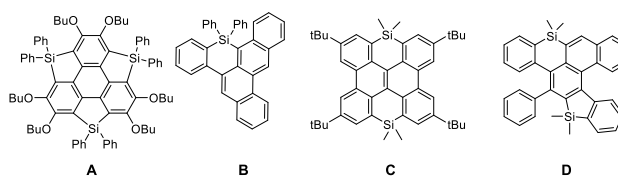
Fig. 1: Examples of Si-containing PAHs **A-D** reported in the literature

To develop novel Si-containing PAHs, we decided to adapt the Ru-catalyzed annulation described by Fukuzawa *et al.*[18] toward the preparation of PAH featuring two Si-atoms and investigate the optical/redox properties and device incorporation of the novel derivatives generated in that way. Using commercial starting materials that we previously used to prepare polyaromatic bisphosphoniums,[19] we synthesized in one step the corresponding dimethylsilane **1a** (Scheme 1). **1a** was then engaged in the Ru-catalyzed cyclization with diphenylacetylene.[18] The resulting disilapyrene **2a** was obtained in moderate isolated yield, because of purification difficulties. **2a** was fully characterized (see ESI). To illustrate that this strategy allows for easy molecular engineering, various polyaromatic bis-silanes were converted into the corresponding disilapyrene **3** (isomer of **1a**) and disilanthrathene **4** in good yields (Scheme 1).[20] The exocyclic Si-substituent could also be modified (from Me to Ph) with the preparation of **2b**. In contrast to the reports based on the annulation of only one Si-cycle, the use of electron-rich or electron-poor alkyne led to uncomplete cyclization products only (see Scheme S1 and Fig S12). However, this approach allowed us to prepare a novel family of Si-doped PAHs **2-4** with variable π-extension and Si-substituents. All compounds are perfectly air and moisture stable and display good solubility in classical organic solvents.
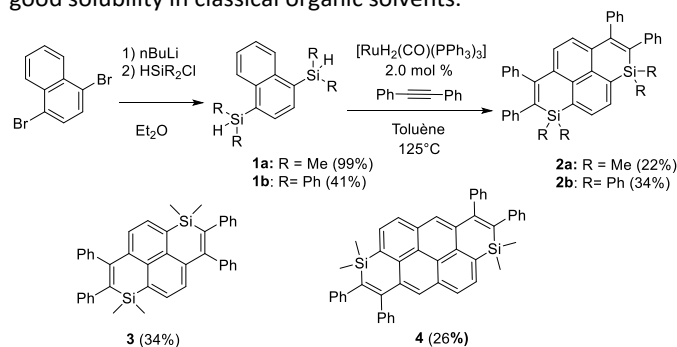
Scheme 1: Synthetic access to **2a-b** and chemical structure of compounds **3-4**

The structures of **2a, 2b** and **4** were confirmed by single-crystal X-ray diffraction (Fig. 2).[21] In all compounds, the Si-atom shows a classical tetrahedral shape with usual valence angles and bond lengths (Table S2). The C-sp^2 skeleton including the heterocycles is mainly planar (maximum deviation from the mean C-sp^2 plane between 0.08 Å for **2a** and 0.19 Å for **2b**, Fig. 2), and the peripheral phenyls lie perpendicularly to this plane. These structural characteristics are conserved in solution according to DFT calculations (Fig. S15). No intermolecular interactions were observed in the crystal packing, likely due to the presence of tetrahedral Si-atoms and the steric hindrance of the peripheral phenyls. Such property is beneficial for the design of sold-state emitters.

The optical properties (absorption/emission) of **2**-**4** have been investigated in diluted DCM solutions (c = 5.10^{-6} mol.L^{-1}, Fig. 3 and Table 1).[21] They all display structured absorption bands in 340-440 nm range, classical for PAHs derivatives. This absorption is attributed to a delocalized π-π* transition with limited Si contributions according to TD-DFT calculations (Figs 3 and S16). Both endo- and exo-skeletal modifications have minor impact on the absorption properties. However, as observed in the silole series, a small red-shift occurs when Me substituents of **2a** are replaced by Ph in **2b**, due to negative hyperconjugation within the Si ring (Fig. S16).[22] Moreover, one notices in Fig. S16 that the central carbon atoms are not involved in the transition in **2**, contrary to **3** and **4**. In addition in **4**, we notice that the excitation is mostly centred on the four central phenyl rings,

whereas the Si-containing rings play a significantly stronger role in **2** and **3**.

2-**4** are also emissive in diluted solution in the 400-600 nm range. As can be seen in Table S3, there is an excellent agreement between the experimental and theoretical 0-0 energies. While the optical properties of **2a** and **3** are very similar, we notice a slight red-shift of the emission for **2b**, and more importantly, a blue shifted emission for **4** (Table 1). This is somewhat surprising as **4** is the most π-extended derivative and as the position of the absorption peak is not strongly displaced as compared to the other systems. Interestingly, theory accurately reproduces these trends (Table S3), including the much smaller Stokes shift of **4** as compared to the other derivatives. Fig. S17 allows to rationalize this behaviour: the ground and excited state geometries are extremely similar in **4**, but significantly different in, e.g., **2a**, consistent with the experimental trends in Stokes shifts. All compounds display low to moderate photoluminescence quantum yields in solution (2 % < φ < 25 %). As expected, **2**-**4** are fluorescent in powder (Fig S14 and Table 1) and the trend for the emission wavelengths in powders parallels the one found in solution. Luminescence quantum yields are considerably increased (19-35%, with the maximum value for **2b**) compared to the diluted solution. Such behaviour was previously observed on our related polyaromatic bisphosphoniums[19] and can be rationalized on the basis of the rotation restriction of the peripheral phenyl rotors.
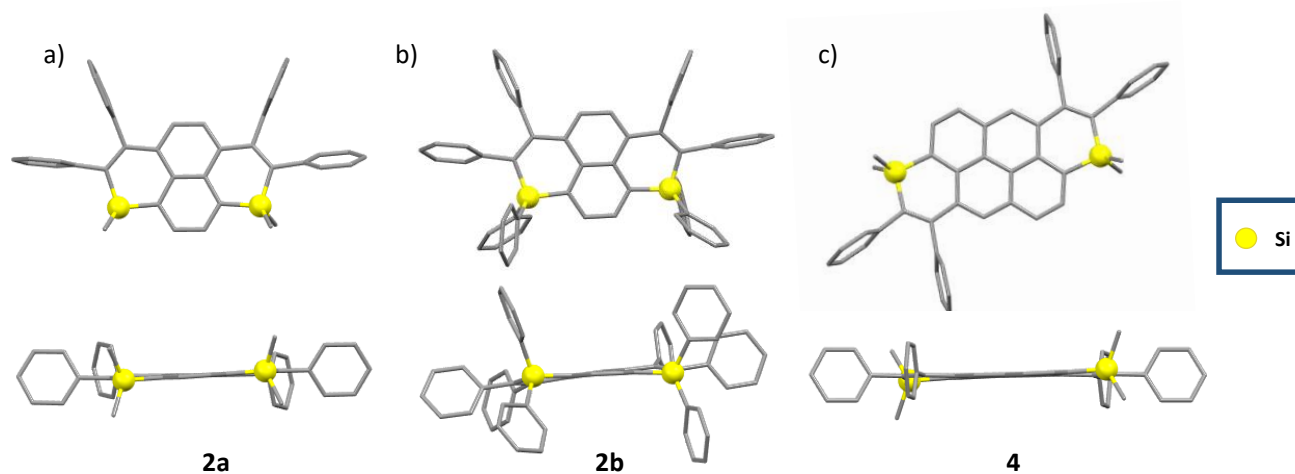
Fig. 2: X-ray crystallographic structure of **2a, 2b** and **4** in top view (up) and lateral view (down)
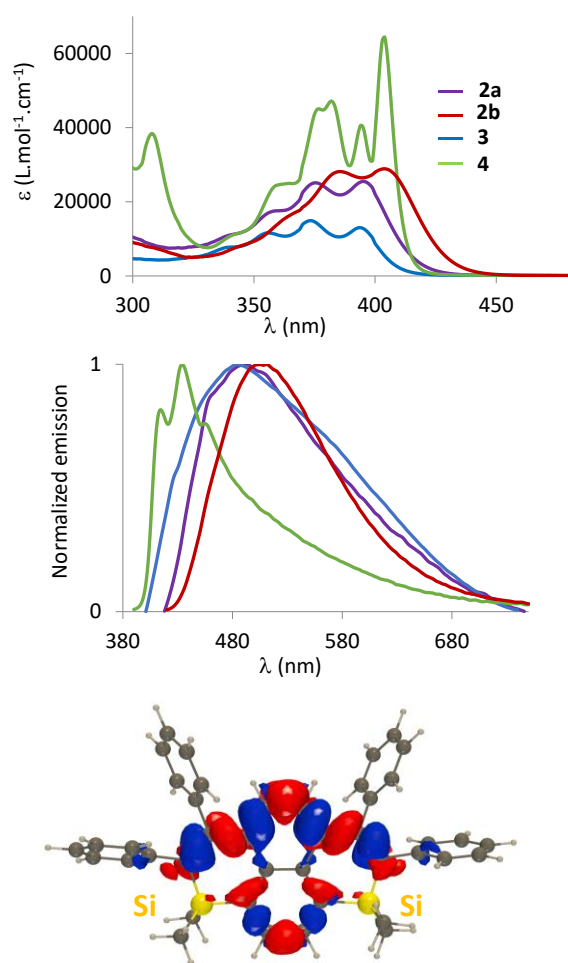
Fig. 3. UV-Vis absorption (up) and normalized emission spectra (middle) of **2-4** in DCM (c = 5.10^{-6} M). Electron density difference computed for **2a** (down). The blue and red regions respectively indicate the decrease and increase of electron density upon photon absorption (contour threshold: 8 10^{-4}).

The redox properties of **2-4** were investigated by cyclic voltammetry in DCM. All derivatives display one quasi-reversible oxidation wave (for example, E_{ox}(**2a**)= +0.88 V vs Fc, Table 1). No reduction is observed in these experimental conditions. As expected, the use of more π-extended structure in **4** (E_{ox}(**4**)= +0.83 V vs Fc, Table 1). or richer group on the Si-atom (Me in **2a** *vs* Ph in **2b** (E_{ox}(**2b**)= +0.95 V vs Fc, Table 1) allows decreasing the oxidation potential. We also underline that the redox behavior of these compounds markedly differs compared previously reported B- and P-analogs featuring similar carbon domains,[19,23] which were strong electron acceptors. This nicely illustrates how one can tune the redox properties by modifying the main group element of heteroatom-doped PAHs.

Considering its thermal stability (td$_{10}$ = 411°C, Fig. S18) associated with favourable electronic properties (*vide supra*), **2a** was used as emitter in a classical multilayer Organic Light-Emitting Diode (OLED) architecture (Glass / ITO / CuPc (10 nm) / α-NPB (40 nm) / TcTa (10 nm) / EML (20 nm) / TPBi (50 nm) / LiF (1.2 nm) / Al (100 nm), see ESI for details). Devices performances are reported in Table S4 and Fig. S19. When **2a** is used as dopant in a mCP host matrix (doping rate 1.7 % w), the electroluminescence resembles the one of the diluted solution (λ^{EL} = 460 nm), with a turn on voltage V_{on} of 4.16 V and a moderate external quantum efficiency (EQE) of 1.1% (Table S4). Non-quantitative energy transfer from the matrix is evidenced by the presence of residual mCP emission at high energy (Fig. S19). However, even when the doping rate was increased to 10%, complete energy transfer was not observed (Fig. S19). In all these devices, the performances (V_{on}, EQE, brightness) are in the same order of magnitude. In order to improve the efficiency, a comprehensive study using various matrices and doping rates would be necessary. Such study appears however beyond the scope of the current work. Nevertheless, these promising preliminary experiments illustrate that Si-containing PAHs such **2a** can be used in electroluminescent devices.

Table 1: Optical and electrochemical data

	λ_{abs}[a] (nm)	ε [a] (L.Mol^{-1}.cm^{-1})	λ_{em} [a] (nm)	ϕ[a,b] (%)	σ (cm^{-1})	λ_{em} [c] (nm)	ϕ[b,c] (%)	E_{ox} [d] (V vs Fc)
2a	395	25500	480	6	4483	446	19	+ 0.88
2b	404	28900	499	25	4712	467	35	+ 0.95
3	396	14900	485	2	4634	446	29	+ 0.97
4	404	64200	435	10	1764	437	27	+ 0.83

[a] In CH$_2$Cl$_2$ (10^{-5}M). [b] Measured in calibrated integration sphere [c] Measured in powder [d] (c = 10^{-3} M) recorded in CH$_2$Cl$_2$ with Bu$_4$N$^+$PF$_6^-$(0.2 M) at a scan rate of 200 mVs^{-1}. Potentials vs Fc$^+$/Fc.

In this communication, the straightforward synthesis of Si-containing PAHs **2-4** using a Ru-catalyzed synthetic approach was reported. The impact of π-extension and exocyclic modifications on the optical (absorption and emission) and redox properties has been investigated and rationalized using a joint experimental/theoretical approach. Finally, one compound with satisfying luminescence properties and thermal stability was selected to prepare an OLED device. Finally, this work highlights the potential of Si-doped PAHs for optoelectronic applications and paves the way toward the preparation of functional Si-containing nanographenes.

1 M. D. Watson, A. Fechtenkotter and K. Müllen, *Chem. Rev*. 2001, **101**, 1267; J. S. Wu, W. Pisula and K. Müllen, *Chem. Rev*. 2007, **107**, 718.

2 A. Narita, X. Y. Wang, X. Feng and K. Müllen, *Chem. Soc. Rev.*, 2015, **44**, 6616.

3 K. Kawasumi, Q. Zhang, Y. Segawa, L. T. Scott and K. Itami, *Nat. Chem.* 2013, **5**, 739; b) W. Zeng, T. Y. Gopalakrishna, H. Phan, T. Tanaka, T. S. Herng, J. Ding, A. Osuka and J. Wu, *J. Am. Chem. Soc.* 2018, **140**, 14054.

4 M. Stępień, E. Gońka, M. Żyła and N. Sprutta, *Chem. Rev.* 2016**, 117**, 3479–3716.

5 Z. Zhou, A. Wakamiya, T. Kushida, S. Yamaguchi, *J. Am. Chem. Soc.* 2012, *134*, 4529-4532; V. M. Hertz, M. Bolte, H.-W. Lerner and M. Wagner, *Angew. Chem. Int. Ed.*, 2015, **54**, 8800.

6 S. M. Draper, D. J. Gregg and R. Madathil, *J. Am. Chem. Soc.* 2002, *124*, 3486-3487.

7 L. Đorđević, C. Valentini, N. Demitri, C. Mézière, M. Allain, M. Sallé, A. Folli, D. Murphy, S. Mañas-Valero, E. Coronado and D. Bonifazi, *Angew. Chem. Int. Ed*., 2020, **59**, 4106.

8 R. Szűcs, P.-A Bouit, L. Nyulászi and M. Hissler, *ChemPhysChem* 2017, **18**, 2618.

9 a) T. Baumgartner, F. Jaekle (Eds), Main Group Strategies toward Functional Hybrid Materials, **2018**, John Wiley & Sons (UK); b) E. Hey-Hawkins, M. Hissler (Eds), Smart Inorganic Polymers , **2019**, John Wiley & Sons (UK).

10 a) M. Hissler, P. W. Dyer and R. Réau, Coord. Chem. Rev. 2003, **244**, 1. b) X. Zhan, S. Barlow and S. R. Marder, Chem. Commun. 2009, 1948.

11 S. Yamaguchi, S. Akiyama and K. Tamao *J. Am. Chem. Soc.* 2000, **122**, 6793.

12 B. Su, A. Kostenko, S. Yao and M. Driess *J. Am. Chem. Soc*. 2020, **142**, 16935–16941

13 T. Nukazawa and T. Iwamoto*, J. Am. Chem. Soc.* 2020, **142**, 9920.

14 S. Furukawa, J. Kobayashi and T. Kawashima, *J. Am. Chem*. *Soc.* 2009, **131**, 40, 14192.

15 a) T. Tsuda, Y. Kawakami, S.-M. Choi and R. Shintani, *Angew. Chem. Int. Ed.*, 2020, **59**, 8057; b) Y. Tokoro and T. Oyama, *Chem. Lett*. 2018, **47**, 130.

16 A. Mitake, R. Nagai, A. Sekine, H. Takano, N. Sugimura, K. S. Kanyiva and T. Shibata, *Chem. Sci.* 2019,**10**, 6715.

17 Z. Ma, C. Xiao, C. Liu, D. Meng, W. Jiang and Z. Wang, *Org. Lett*., 2017, **19**, 4331.

18 Y. Tokoro, K. Sugita and S. Fukuzawa, *Chem. Eur. J.*, 2015, **21**, 13229.

19 a) T. Delouche, A. Vacher, E. Caytan, T. Roisnel, B. Le Guennic, D. Jacquemin, M. Hissler and P.-A. Bouit, *Chem. Eur. J.* 2020, **26**, 8226-8229 ; b) T. Delouche, A. Vacher, T. Roisnel, M. Cordier, J-F. Audibert, B. Le Guennic, F. Miomandre, D. Jacquemin, M. Hissler and P-A. Bouit, *Mater. Adv.,* 2020, **1**, 3369-3377.

20 Alternative synthetic approach to **3**, see: T. Saeki, A. Toshimitsu and K. Tamao, *J. Organomet. Chem*. 2003, **1**, 215.

21 The X-ray structure and optical properties in solution of **3** has been described in reference 20.

22 H. Chen, M. Denis, P.-A. Bouit, Y. Zhang, X. Wei, D. Tondelier, B. Geffroy, Z Duan and M. Hissler, *Appl. Sci.* **2018**, *8*, 812.

23 J. M. Farrell, C. Mützel, D. Bialas, M. Rudolf, K. Menekse, A.-M. Krause, M. Stolte and F. Würthner, *J. Am. Chem. Soc.* 2019, *141*, 9096.